J Appl Electrochem (2008) 38:1259–1267
DOI 10.1007/s10800-008-9550-2

ORIGINAL PAPER

Effect of leakage currents on the secondary current distribution in bipolar electrochemical reactors

E. R. Henquín · J. M. Bisang

Received: 5 December 2007 / Revised: 7 March 2008 / Accepted: 10 March 2008 / Published online: 1 April 2008

Abstract The secondary current distribution in an electrochemical stack with one bipolar electrode was experimentally determined and compared with the theoretical prediction according to the Laplace equation. A close agreement between both results is reported. The parameters acting upon the current distribution were lumped into a dimensionless variable, called the bipolar Wagner number, and its effect on the current distribution and predictive suitability of the theoretical treatment is discussed.

Keywords Bipolar electrodes · Current distribution · Electrochemical reactors · Laplace equation · Leakage current

List of symbols

a_i	Constants in Eq. 9
A	Transverse section of the electrolyte manifold (m^2)
b_i	Tafel slope of the ith reaction (V)
d_r	Mean relative deviation given by Eq. 16 (%)
D	Weighting factor in Eq. 11
E_0	Reversible electrode potential (V)
G	Length of the electrolyte manifold (m)
h	Distance between two nodes in the potential grid (m)
$j_{i,k}$	Current density of the ith reaction (i = a or c) at the kth electrode (k = A, B or C) (A m^{-2})
j_{mean}	Mean current density (A m^{-2})
j_0	Exchange current density (A m^{-2})
I	Total current (A)
I^*	Leakage current (A)
I_B	Total current at the bipolar electrode (A)
L	Electrode length (m)
n	Number of bipolar electrodes
N	Number of experimental values in Eq. 16
R	By-pass resistance (Ω)
Tol	Tolerance of the calculation
U	Applied voltage to the reactor (V)
U_0	Reversible cell voltage (V)
W	Electrode width (m)
Wa_{Bi}	Bipolar Wagner number
x	Axial coordinate (m)
y	Axial coordinate (m)

Greek characters

η	Overpotential (V)
ρ	Electrolyte resistivity (Ω m)
σ	Standard deviation
ϕ	Potential (V)
ϕ_0	Potential in the solution phase adjacent to an electrode surface (V)

Subscripts

a	Anodic reaction
c	Cathodic reaction
exp	Experimental value
m	Metal phase
s	Solution phase
th	Theoretical value
A	Terminal anode
B_k	kth bipolar electrode
C	Terminal cathode

Superscript

r	iteration number

E. R. Henquín · J. M. Bisang (✉)
Programa de Electroquímica Aplicada e Ingeniería Electroquímica (PRELINE), Facultad de Ingeniería Química (UNL), Santiago del Estero 2829, S3000AOM Santa Fe, Argentina
e-mail: jbisang@fiq.unl.edu.ar

1 Introduction

Bipolar electrochemical reactors are attractive devices for industrial processes due to their simple construction. However, this advantage is counteracted by the existence of leakage currents, which cause a decrease in current efficiency, current distribution along the electrodes and the possibility of corrosion zones in the reactor. The authors have previously proposed a simplified model to predict the effect of the leakage current on the current distribution [1]. In [2] the primary current distribution obtained by the numerical solution of the Laplace equation was reported and compared with experimental results. The state of the art related to bipolar electrochemical reactors has recently been described [1, 2]. Some authors have analyzed particular aspects of these devices. Thus, Jupudi et al. [3] reported a model to calculate the leakage current in a bipolar stack with dual electrolyte inlets, with special attention to the importance of the individual resistance components of the cell. The presence of gases in the outlet manifolds was considered, Tafelian kinetics was adopted at the electrodes and uniform current distributions along the electrodes were assumed. Furthermore, Kodým et al. [4] reported experimental and theoretical results of potential and current distribution in a bipolar system. The special configuration of the electrochemical reactor allowed for the simulation of the current distribution along the electrode thickness and the identification of the electrode ends as the most active regions of the bipolar electrode. Kodým et al. [5] also reported a mathematical optimization of the geometry of a bipolar stack applied to the direct drinking water disinfection.

The aim of this work is to analyse the effect of leakage currents on the secondary current distribution at the electrodes in an undivided bipolar stack by numerical solution of the Laplace equation, and to compare the theoretical results with experimental ones.

2 Theoretical considerations

The bipolar electrochemical stack considered in this paper consists of a series of identical reactors. Each reactor is in the form of a horizontal channel of a rectangular cross section with vertical electrodes. Each inside reactor of the stack is composed of the anodic side of a bipolar electrode, the cathodic side of the next bipolar electrode and between them the electrolyte without an electrode separator. The outermost reactors of the stack include the terminal anode A or the terminal cathode C. Each reactor has manifolds for the inlet and outlet of the electrolyte, which generate leakage currents. In the following mathematical treatment some simplifying assumptions are made:

(i) The metal phase of the electrodes is isopotential.
(ii) The current distribution in the direction of the electrode width is neglected.
(iii) The effect of the gases generated at the electrodes on the electrolyte resistivity is disregarded due to the special configuration of the stack.
(iv) Only one half of the reactor is considered for the sake of symmetry.

Thus, in order to obtain the potential distribution, it is necessary to solve the Laplace equation in the solution phase including the electrolyte manifolds:

$$\frac{\partial^2 \phi_s(x,y)}{\partial x^2} + \frac{\partial^2 \phi_s(x,y)}{\partial y^2} = 0 \tag{1}$$

subject to the following boundary condition at the electrode surfaces:

$$\left.\frac{\partial \phi_s(x,y)}{\partial x}\right|_{\text{i th electrode surface}} = -\rho\, j_{i,k}(y) \tag{2}$$

where i represents the anodic or the cathodic reaction at the kth electrode. Assuming a Tafel equation for the kinetics at each electrode surface is

$$j(y) = j_0 \exp\left[\frac{\eta(y)}{b}\right] \tag{3}$$

being

$$\eta(y) = \phi_m - \phi_0(y) - E_0 \tag{4}$$

and at the insulating walls

$$\left.\frac{\partial \phi_s(x,y)}{\partial x}\right|_{\text{insulating walls}} = \left.\frac{\partial \phi_s(x,y)}{\partial y}\right|_{\text{insulating walls}} = 0 \tag{5}$$

The current drained at each electrode surface is given by

$$I_k = W \int_0^L j_{i,k}\,dy \tag{6}$$

In the case of an electrochemical stack with one bipolar electrode the leakage current is given by

$$I^* = I_{A\,\text{or}\,C} - I_{B_1} \tag{7}$$

Equation 1 was numerically solved by the finite difference method with an equidistant grid taking into account the boundary conditions given by Eqs. 2 and 5. In order to obtain the current density distribution at each electrode surface, the following iteration procedure composed of three iteration loops was used. In the first place the cell voltage, U, was supposed and the potential of the terminal anodic metal phase was calculated as

$$\phi_{m,A} = U - (n+1)U_0 \tag{8}$$

and the primary potential distribution inside the reactor was determined according to the method outlined in [2]. For a

given axial position y along the electrode length, the four potential points in the solution phase nearest to each electrode surface, that is $\phi_s(h, y)$, $\phi_s(2h, y)$, $\phi_s(3h, y)$ and $\phi_s(4h, y)$, were fitted with the polynomial:

$$\phi_s(x, y) = a_0 + a_1 x + a_2 x^2 + a_3 x^3 \quad (9)$$

Taking the derivative of Eq. 9 evaluated at the electrode surface, the current density is given by:

$$j(y) = \frac{1}{\rho} \left. \frac{\partial \phi_s(x, y)}{\partial x} \right|_{\text{electrode surface}} = \frac{a_1}{\rho} \quad (10)$$

Combining Eqs. 3, 4 and 10 the solution potential adjacent to each electrode surface, called surface potential $\phi_0(y)$, was calculated. Introducing $\phi_0(y)$ into Eq. 9, together with the previous values of $\phi_s(2h, y)$, $\phi_s(3h, y)$ and $\phi_s(4h, y)$, new values of the parameters a_0, a_1, a_2 and a_3 were obtained. Thus, a new potential at the node nearest to each electrode surface, $\phi_s(h, y)$, was calculated and introduced in the potential grid being the potential distribution inside the reactor re-calculated. This procedure was repeated until the new value of current density at each axial position agreed with the previous one. For some experiments, in order to obtain convergence in this iteration, it was necessary to use an attenuated value of potential at the node nearest to each electrode surface according to [6]

$$\phi_s^{r+1}(h, y) = \phi_s^{r-1}(h, y) + D \left[\phi_s^{r}(h, y) - \phi_s^{r-1}(h, y) \right] \quad (11)$$

where D is a weighting factor which varies between 0 and 1. A common value for D was 0.7. When the iteration for the calculation of the current densities matched a specified error criterion, the current at the terminal electrodes was evaluated with Eq. 6. If the calculated current disagreed with the experimental one, a new value for the applied potential to the reactor was proposed and a new iteration loop was performed. The applied voltage was updated following a linear relationship with the current. When the potential-current iteration met the convergence criterion the current at the bipolar electrode was calculated with Eq. 6 and the leakage current with Eq. 7. The by-pass resistance in the modelling was then evaluated as the quotient of the average value of the potential difference between the inlet and outlet of the manifold and the leakage current. The new value of the by-pass resistance was compared with the experimental one, in case of discrepancy the part of the potential grid representing the by-pass resistor was properly modified and a new iteration loop was performed until the convergence criterion was attained. The tolerance of the calculation at each iteration loop was always lower than 0.3%. The calculation procedure is shown in more detail in Fig. 1.

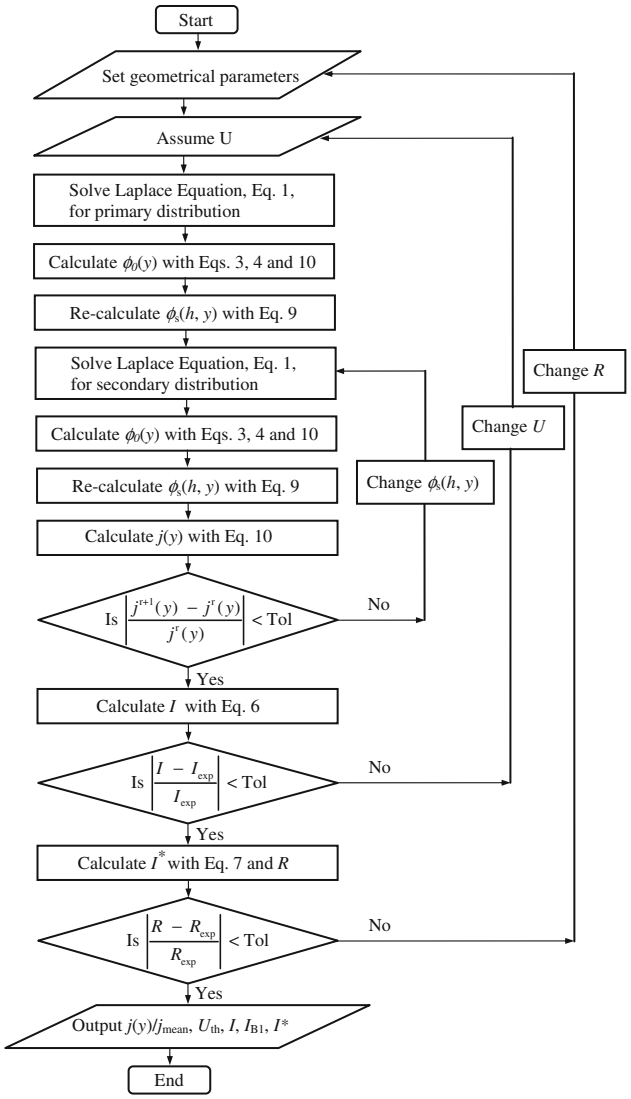

Fig. 1 Flow chart illustrating the calculation procedure

3 Experimental details

The experimental setup was composed of two undivided reactors electrically connected in series, as shown schematically in Fig. 2, which constitutes a bipolar electrochemical stack with one bipolar electrode. For symmetry reasons, only one half of the stack was considered. Thus, the inlet manifold was simulated by a Teflon tube, which interconnects the electrolyte in the reactors. With the aim of searching for the effect of the by-pass resistance four types of Teflon tubes, whose geometrical dimensions are given in Table 1, and two different electrolyte concentrations were used. Hence eight by-pass resistances ranging from 19.32 Ω to 363.38 Ω were examined. The current density distribution was determined using the segmented electrode method, and hydrogen- and

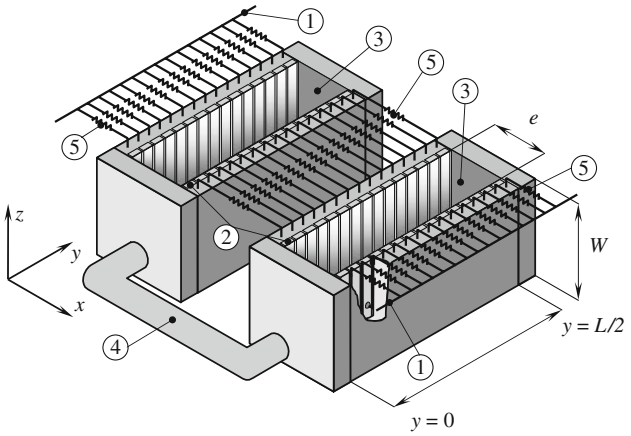

Fig. 2 Schematic representation of the bipolar electrochemical stack. 1, current feeder of the terminal electrodes; 2, bipolar electrode; 3, interelectrode gap; 4, electrolyte manifold; 5, calibrated resistors

Table 1 Geometrical parameters of the by-passes

Type	$A \times 10^{-4}$ (m^2)	G (m)
I	0.283	0.184
II	0.739	0.189
III	1.887	0.208
IV	2.986	0.196

Table 2 Physicochemical properties and kinetic parameters used in modelling

ρ [NaOH] = 1 M (Ω m)	5.59×10^{-2}
ρ [NaOH] = 3 M (Ω m)	2.94×10^{-2}
U_0 (V)	1.23
b_a (V)	0.0435
$j_{0,a}$ (A m^{-2})	1×10^{-3}
b_c (V)	0.0391
$j_{0,c}$ (A m^{-2})	1×10^{-1}

oxygen-evolution from 1 M NaOH or 3 M NaOH were the cathodic and anodic reactions. Table 2 summarizes the physicochemical properties and the kinetic parameters used in the modelling. The electrodes at each reactor were formed with 15 nickel segments, 6.1×10^{-3} m wide and 0.05 m high, which were insulated from one another by an epoxy resin of about 5×10^{-4} m thick. The interelectrode gap was 0.02 m and the segments were trimmed to make a reactor of 0.1 m in length. Calibrated resistors made from constantan wire, 0.1 m long, 1.5×10^{-3} m diameter and a resistance of about 0.02 Ω, were inserted between the backside of each segment and the current feeder at the terminal electrodes and between the backside of the corresponding anodic and cathodic segments at the bipolar electrode. The current distribution at each electrode was determined by measuring the ohmic drop in the resistor. The effect of the calibrated resistors on the current distribution can be neglected due to the small value of their resistance in comparison with that of the electrolyte. The data acquisition was performed using a computer controlled, home made analogue multiplexer. A dc power supply was used to apply a constant current to the feeders. The electric connection was made at three points, in the middle and at both ends, of the current feeder of each terminal electrode. The temperature in all experiments was approximately 30 °C.

4 Results and discussion

Figure 3 presents the potential distribution in the reactor for a typical case, where an abrupt change in potential is observed at each electrode surface, and an approximately linear variation in potential in the interelectrode gap is detected for the region farther from the by-pass. In the proximity of the by-pass the variation in potential is altered by the leakage current. Figure 4 shows the effect of the by-pass resistance on the secondary current distribution at the terminal electrodes for an electrochemical stack with one bipolar electrode. The symbols • correspond to the mean value of three independent measurements performed at each terminal electrode. Likewise, the symbols × represent mean values of current distribution when the reactor was operated without a by-pass of electrolyte. In both cases the standard error is given by the vertical segments. The full lines show the theoretical secondary current distribution. For the calculation of the theoretical curves, the kinetic parameters of the anodic and cathodic reactions have been taken from literature [7, 8]. Therefore these data are only approximate and the exchange current density poses considerable uncertainty because of the roughness

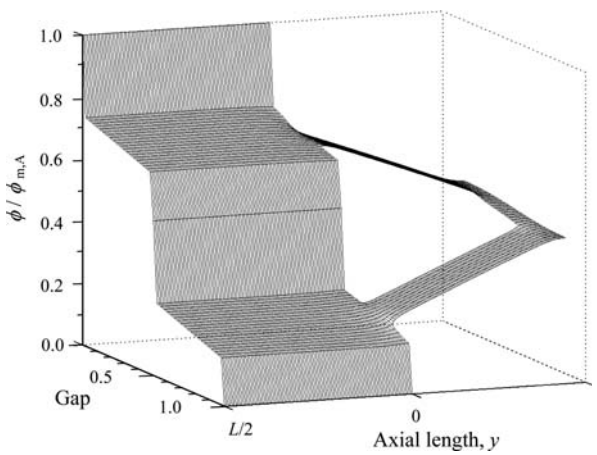

Fig. 3 Secondary potential distribution for an electrochemical stack with one bipolar electrode. Correspond to the case reported in Fig. 4d

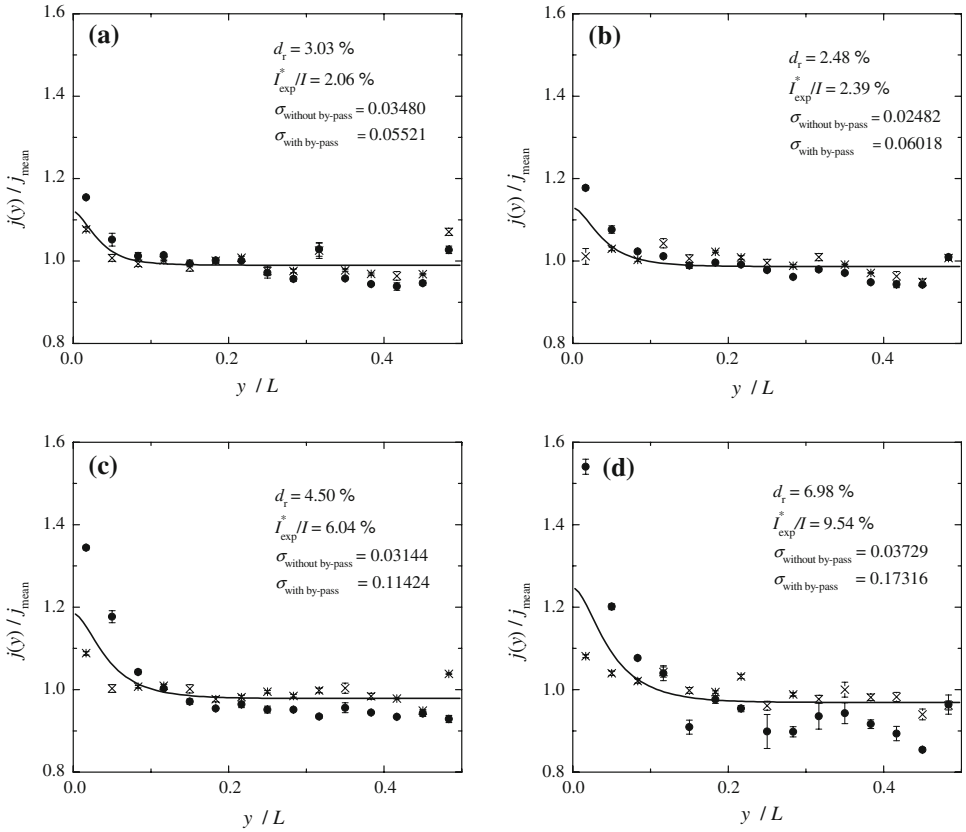

Fig. 4 Current distributions in the terminal electrodes for different values of the by-pass resistance. One bipolar electrode. (**a**) $R = 191.20\ \Omega$ (**b**) $R = 75.41\ \Omega$ (**c**) $R = 32.36\ \Omega$ and (**d**) $R = 19.32\ \Omega$. ×—Current distribution without by-pass; •—Current distribution with by-pass; Vertical segments—standard error; Full line—theoretical prediction. I = 1A, [NaOH] = 3 M

factor of the electrode. However, its influence on the applied voltage and leakage current is irrelevant; for example, a variation of one magnitude order in the anodic exchange current density causes only a change of about 2.4% in U and I^*, but it has no effect on the current distribution curve. The standard deviation of the experimental current distributions related to the mean current density is also included as a figure of merit to quantify the experimental current distribution. Thus, a high value of standard deviation means that the current distribution is less uniform. As expected, the standard deviations of the experimental measurements without an electrolyte by-pass are lower than those with a by-pass. When a by-pass is considered, the most important variation in the current density occurs at the end of the electrode, because the region near the inlet of the electrolyte mainly contributes to the leakage current. Likewise, when the by-pass resistance decreases the current distribution is more pronounced, higher values of standard deviation, which is related to the increase in the leakage current.

Similarly, Fig. 5 shows current distributions for different total currents. Comparing part (a) with part (b) and part (c) with part (d), it is observed that more uniform distributions are obtained when the total current increases. This behaviour can only be detected for secondary current distribution and it may be associated with the increase of the fraction of current drained through the by-pass when the current decreases. Thus, when the total current diminishes the polarization resistance rises and it facilitates a higher value of leakage current. Also, the comparison of Fig. 5d with Fig. 5a and of Fig. 5c with Fig. 4b shows the effect that the electrolyte resistivity has on the current distribution. Thus, a decrease in resistivity, a more concentrated electrolyte, generates an increase in the current distribution because the by-pass resistance lowers.

Typical curves of current distribution at the bipolar electrode for some cases reported in Figs. 4 and 5 are given in Fig. 6. The experimental current distributions at the bipolar electrode are more uniform than at the terminal electrodes, which corroborates the tendency also observed for the primary case [1, 2]. However, an important variation in the current density takes place in the first segment near the manifold, which disagrees with the theoretical model and can be attributed to a change in effective electrolyte resistance due to the gas evolved at the electrodes.

According to Figs. 4–6 the current distribution depends on the geometric characteristics of the electrolyte manifold, the resistivity of the electrolyte and the applied current to the reactor. Thus, taking into account ρ, $d\eta/dI$ as electrochemical parameters and A/G as the characteristic length of the manifold and performing a dimensional analysis, gives the following dimensionless number

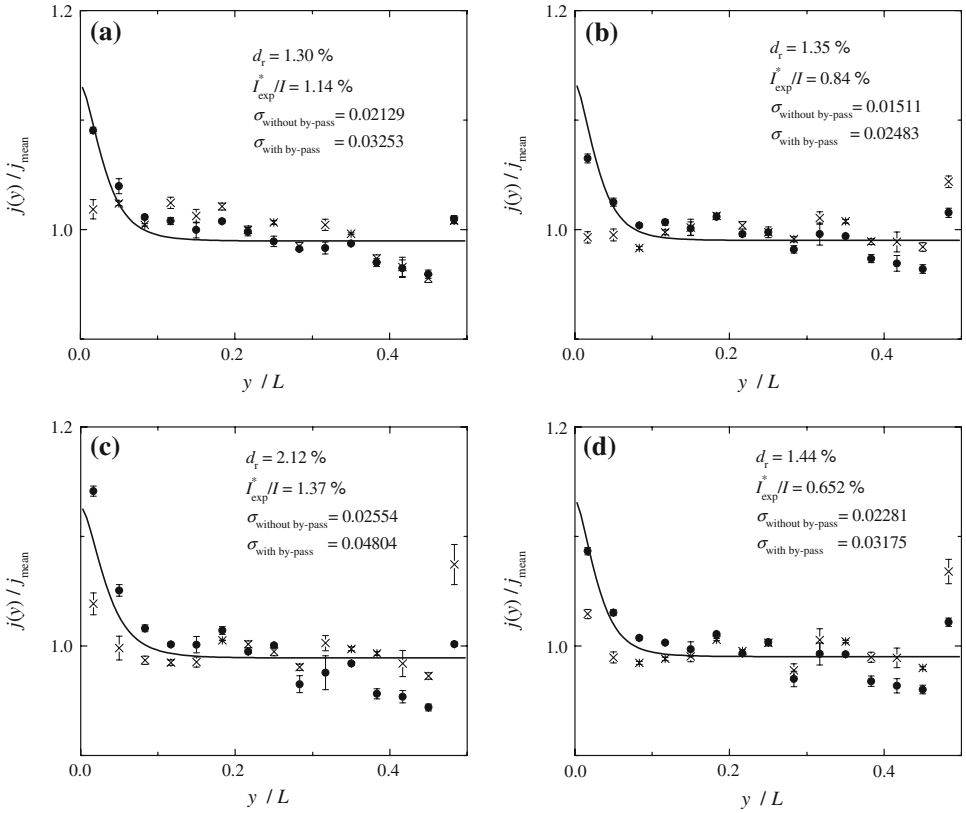

Fig. 5 Current distributions in the terminal electrodes for different values of total current. One bipolar electrode. (**a**) I = 3 A, [NaOH] = 3 M, $R = 75.41\ \Omega$ (**b**) I = 5 A, [NaOH] = 3 M, $R = 75.41\ \Omega$ (**c**) I = 1 A, [NaOH] = 1 M, $R = 143.33\ \Omega$ and (**d**) I = 3 A, [NaOH] = 1 M, $R = 143.33\ \Omega$. ×—Current distribution without by-pass; •—Current distribution with by-pass; Vertical segments—standard error; Full line—theoretical prediction

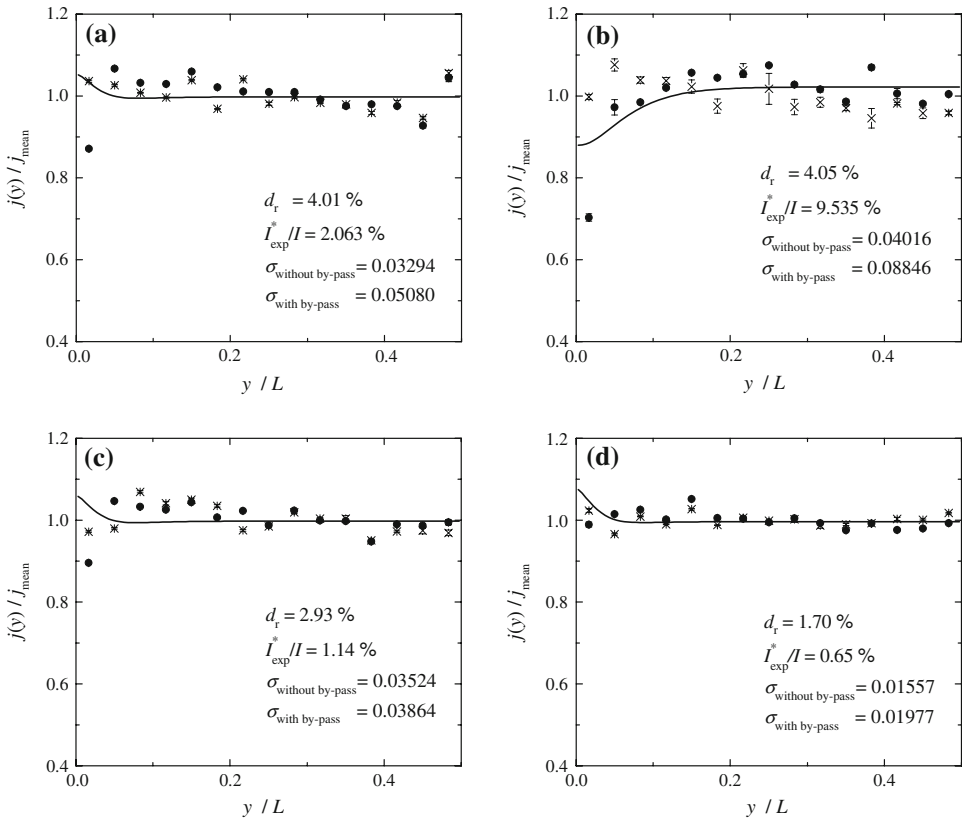

Fig. 6 Current distributions in the bipolar electrode. One bipolar electrode. (**a**) I = 1 A, [NaOH] = 3 M, $R = 191.20\ \Omega$ (**b**) I = 1 A, [NaOH] = 3 M, $R = 19.32\ \Omega$ (**c**) I = 3 A, [NaOH] = 3 M, $R = 75.41\ \Omega$ and (**d**) I = 3 A, [NaOH] = 1 M, $R = 143.33\ \Omega$. ×—Current distribution without by-pass; •—Current distribution with by-pass; Vertical segments—standard error; Full line—theoretical prediction

Table 3 Summary of experimental results for one bipolar electrode

[NaOH]	R (Ω)	I (A)	d_r (%)		$\sigma \times 10^2$		$Wa_{Bi} \times 10^5$		Theor.	Exp.
			Terminals	Bipolar	Terminals	Bipolar				
1 M	363.38	0.996	2.67	1.80	4.871	2.569	22.82	U (V)	6.62	6.47
								I^* (mA)	5.7	9.2
		2.970	2.10	1.78	3.578	2.244	7.65	U (V)	11.44	10.30
								I^* (mA)	12.1	14.2
		5.107	2.05	1.19	4.545	2.383	4.45	U (V)	16.13	15.62
								I^* (mA)	18.6	47.2
	143.33	0.978	2.12	2.07	4.804	2.862	58.90	U (V)	5.35	5.23
								I^* (mA)	9.9	13.4
		2.967	1.44	1.70	3.175	1.977	19.42	U (V)	7.88	7.74
								I^* (mA)	18.6	19.4
		4.957	1.40	1.60	2.327	1.674	11.63	U (V)	10.26	10.08
								I^* (mA)	26.5	30.1
	61.51	0.988	3.01	6.42	8.689	7.929	135.88	U (V)	5.09	4.78
								I^* (mA)	20.4	34.7
		2.967	1.80	3.27	5.843	4.152	45.25	U (V)	7.15	6.83
								I^* (mA)	36.7	45.4
		4.967	1.32	5.09	4.479	7.775	27.03	U (V)	9.08	8.67
								I^* (mA)	51.7	57.9
	36.72	0.998	4.38	4.02	11.43	6.184	225.41	U (V)	4.95	4.71
								I^* (mA)	31.9	50.0
		2.982	2.86	5.69	7.000	11.47	75.42	U (V)	6.66	6.60
								I^* (mA)	54.4	62.2
		4.974	2.81	5.05	6.092	9.764	45.21	U (V)	8.28	8.17
								I^* (mA)	75.51	81.40
3 M	191.20	1.012	3.03	4.01	5.521	5.080	42.70	U (V)	5.57	5.11
								I^* (mA)	8.0	20.9
		2.968	2.33	3.20	4.250	3.953	14.55	U (V)	8.18	7.50
								I^* (mA)	14.6	38.4
		5.085	2.48	1.80	4.829	2.763	8.49	U (V)	10.67	9.91
								I^* (mA)	21.2	62.4
	75.41	0.976	2.48	2.68	6.018	4.020	112.26	U (V)	4.83	4.52
								I^* (mA)	15.4	23.3
		2.962	1.30	2.93	3.253	3.864	36.97	U (V)	6.25	5.89
								I^* (mA)	24.5	33.9
		4.949	1.35	2.75	2.483	3.475	22.13	U (V)	7.54	7.06
								I^* (mA)	33.1	41.7
	32.36	0.991	4.50	8.49	11.42	11.01	257.47	U (V)	4.69	4.31
								I^* (mA)	32.6	59.9
		2.970	1.97	6.45	6.794	9.890	85.93	U (V)	5.85	5.51
								I^* (mA)	50.2	76.9
		4.964	1.02	7.47	4.658	13.22	51.41	U (V)	6.90	6.40
								I^* (mA)	65.9	85.1
	19.32	0.994	6.98	4.05	17.32	8.846	429.85	U (V)	4.59	4.26
								I^* (mA)	51.9	94.8
		2.969	4.00	4.38	9.718	7.435	143.94	U (V)	5.57	5.30
								I^* (mA)	76.1	116.4
		4.958	3.06	7.44	6.590	14.80	86.21	U (V)	6.46	6.10
								I^* (mA)	98.3	141.3

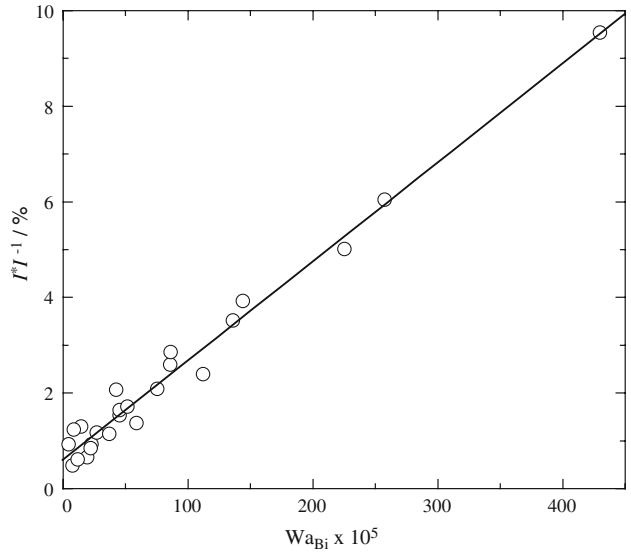

Fig. 7 Fraction of lost current as a function of the bipolar Wagner number

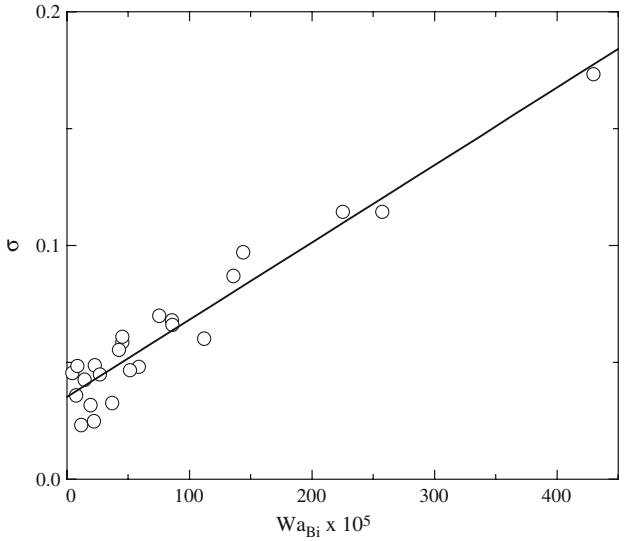

Fig. 8 Standard deviation of the experimental results for the terminal electrodes as a function of the bipolar Wagner number

$$\mathrm{Wa_{Bi}} = \frac{\mathrm{d}\eta/\mathrm{d}I}{\rho\ G/A} \tag{12}$$

Assuming Tafelian kinetics at both electrodes gives

$$\frac{\mathrm{d}\eta}{\mathrm{d}I} = \frac{(b_a + b_c)}{I} \tag{13}$$

Taking into account that the by-pass resistance is given by

$$R = \frac{\rho\ G}{A} \tag{14}$$

Introducing Eqs. 13 and 14 into Eq. 12 yields

$$\mathrm{Wa_{Bi}} = \frac{(b_a + b_c)}{IR} \tag{15}$$

Thus $\mathrm{Wa_{Bi}}$ should be recognized as a bipolar Wagner number which lumps all the parameters conditioning the secondary current distributions at the electrodes. Table 3 summarizes all the experimental results. Figures 4 and 5 and Table 3 show that the current distribution is more significant when the leakage current related to the total current increases and Fig. 7 reports the increase in I^*/I as the bipolar Wagner number increases. Likewise, Fig. 8 shows the standard deviation of the experimental results as a function of the bipolar Wagner number for the terminal electrodes. Contrary to the behaviour of monopolar reactors, an increase in the bipolar Wagner number produces more pronounced current distributions, higher σ values.

Figures 4–6 also make it clear that the experimental and predicted current distributions are in good qualitative agreement. To quantify the predictive capability of the theoretical model the mean relative deviation is introduced as

$$d_r = \frac{1}{N}\sum_{i=1}^{N}\frac{\left|j_{exp}(z_i) - j_{th}(z_i)\right|}{j_{th}(z_i)}\ 100 \tag{16}$$

Lower values of d_r mean a close agreement between both distributions. Figure 9 displays the mean relative deviation between the experimental and theoretical results as a function of the bipolar Wagner number for the terminal electrodes. In general, an acceptable prediction capability of the theoretical treatment, d_r lower than 3%, can be observed. The highest discrepancy is observed for the smaller total current, in which the experimental

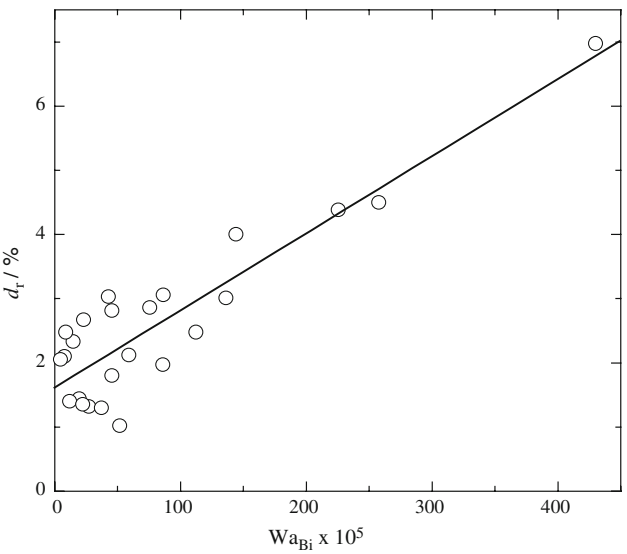

Fig. 9 Mean relative deviation between the theoretical values and the experimental results for the terminal electrodes as a function of the bipolar Wagner number

determination of the current distribution is more difficult due to the small ohmic drop in the calibrated resistors. Furthermore, columns 10 and 11 in Table 3 compare the theoretical and experimental values of cell voltage and leakage current. The experimental leakage currents are always higher than the theoretical ones and the opposite is detected for the cell voltage. The discrepancies observed, mainly in the leakage current prediction, may be attributed to the gases evolved at the electrodes, which increase the effective resistivity of the electrolyte in the interelectrode gap, raising the leakage current. The gases also produce bubble-induced convection altering the hydrodynamics in the solution phase. Both factors may influence the performance of the reactor and they have not been considered in the mathematical modelling.

5 Conclusions

(i) A close agreement for the secondary current distribution in a bipolar electrochemical stack was achieved between experimental results and theoretical calculations obtained from the solution of the Laplace equation considering a Tafel kinetics at the electrodes.

(ii) Some discrepancy in cell voltage and leakage current between experimental and theoretical results can be attributed to the gases evolved at the electrodes, which produce bubble-induced convection of the electrolyte and also variations of the effective electrolyte resistivity inside the reactor.

(iii) As with the primary case, the current distribution is more pronounced at the terminal electrodes than at the bipolar one, which presents only some variation in the entrance region.

Acknowledgements This work was supported by Consejo Nacional de Investigaciones Científicas y Técnicas (CONICET) and Universidad Nacional del Litoral (UNL) of Argentina.

References

1. Henquín ER, Bisang JM (2005) J Appl Electrochem 35:1183
2. Henquín ER, Bisang JM (2007) J Appl Electrochem 37:877
3. Jupudi RS, Zappi G, Bourgeois R (2007) J Appl Electrochem 37:921
4. Kodým R, Bouzek K, Šnita D, Thonstad J (2007) J Appl Electrochem 37:1303
5. Kodým R, Bouzek K, Bergmann H (2007) 58th ISE Annual Meeting
6. Prentice GA, Tobias CW (1982) AIChE J 28:486
7. Tilak BV, Lu PWT, Colman JE, Srinivasan S (1981) In: Bockris JO'M, Conway BE, Yeager E, White RE (eds) Comprehensive treatise of electrochemistry, vol 2, ch 1. Plenum Press, New York
8. Bisang JM (1991) J Appl Electrochem 21:760